Journal of Membrane Science, 40 (1989) 243–260
Elsevier Science Publishers B.V., Amsterdam — Printed in The Netherlands

MASS TRANSFER IN CORRUGATED-PLATE MEMBRANE MODULES. I. HYPERFILTRATION EXPERIMENTS*

M.J. van der WAAL and I.G. RACZ**

University of Twente, Dept. of Chemical Engineering, P.O. Box 217, 7500 AE Enschede (The Netherlands)

Summary

The application of corrugations as turbulence promoters in membrane filtration was studied. This study showed that it is possible to deform an originally flat membrane to a corrugated shape without damaging it. In hyperfiltration experiments using corrugated cellulose acetate membranes it was found that the corrugations improve mass transfer, provided they are not too close together. At a given value of the mass-transfer coefficient, the presence of corrugations can lead to lower energy consumption in hyperfiltration than possible with flat membranes.

Introduction

In membrane filtration processes, as in other filtration processes, components of the incoming feed permeate selectively through the membranes, leaving the rejected components at the feed side of the membrane. The build-up of rejected material near the membrane, called concentration polarisation, results in a decreased rate of permeate production, and, in case the rejection is not complete, in a decreased quality of the permeate.

The decrease in permeate production rate is caused by an increase in osmotic pressure of the feed solution near the membrane, or by accumulation of material which becomes supersaturated near the membrane. In the first case the effective driving force (pressure difference) is reduced, in the latter the hydraulic resistance is increased.

In order to maintain the rate of permeate production and the quality of the permeate the rejected material must be removed from the membranes. This is usually done by leading the feed at some velocity along the membrane. The flow velocity determines the rate of mass transfer between the feed bulk and the membrane wall.

*Paper presented at the Workshop on Concentration Polarization and Membrane Fouling, University of Twente, The Netherlands, May 18–19, 1987.

** To whom correspondence should be addressed.

Given the ratio of permeate to feed volume, the energy consumption of a membrane process is determined by the pressure level at which the process is operated and the required velocity along the membrane. To achieve this velocity, a pressure drop must be overcome. The energy comsumption for leading the flow along the membrane is determined by the product of pressure drop times displaced volume. As an increase in flow velocity results in an increase in pressure drop, whereas in circulation systems the displaced volume increases, the increase in required energy is proportional to the flow velocity to the power 2 and almost 3 for laminar and turbulent flow, respectively. The choice of flow velocity is determined by a balance between cost of membrane area and of energy consumption.

In the literature, methods are described to improve the mass transfer from a membrane wall to the feed flow. These methods include volume displacement rods in tubular membranes [1,2], static mixers in tubular membranes [3–5], small wires attached to or at some distance from the membrane in tubular or flat membranes [6,7], fluidized beds in tubular membranes [8–12] and mesh screens in flat and spiral-wound membranes [13,14]. Most of these techniques cause an increase of mixing in the feed flow near the membrane, thereby decreasing the resistance for mass transfer perpendicular to the membrane. As they stimulate mixing the term "turbulence promoters" is used; however, the flow may still be laminar.

These techniques also cause a frictional pressure drop along surfaces not equipped with membranes, so energy is consumed in passing the fluid along surface which do not produce permeate. Moreover, application of fluidized beds may not only remove a fouling layer from the membrane, but may also damage the membrane as a result of this scouring action.

Membrane filtration installations can be compared with heat-exchangers. Here also an exchange of an entity (heat) from a wall to a flow is desired, whereas fouling of the surface should be prevented. In order to stimulate heat transfer, the same type of methods as given above are applied or investigated. In plate heat-exchangers also corrugated surfaces are applied in different forms [15,16]. These corrugations might increase the mechanical strength of the plates as well as the heat transfer rate.

In this work, results are described of application of corrugations as turbulence promoters. These corrugations are pressed into originally flat membranes. In this first part, results of hyperfiltration experiments using cellulose acetate membranes are described. In the second part, results of ultrafiltration experiments using polysulfone membranes will be given.

The aim of the investigation was to obtain answers to the following questions:

- Can flat membranes be deformed to a predetermined corrugated shape without being damaged?
- Is mass transfer from the membrane wall to the feed bulk influenced positively by the corrugations?

- Can a given value of the mass transfer coefficient be realized using a corrugated membrane wall at a lower energy consumption than using a flat wall?

Preliminary results were published previously [17]. Here, further results are given for mass transfer and hydrodynamics, which combined answer the above questions.

Experimental

Corrugated plates

Corrugations were produced by cutting cylindrical PVC bars of 3 mm diameter in axial direction. These half-cylindrical corrugations were glued on a PVC plate at the desired mutual distances perpendicular to the main flow direction. For hydrodynamic visualisation studies, the plates were colored white to contrast with the applied black ink. Small holes were drilled into the plate to allow permeate to leave the module. At the axial ends of the half-cylinders it was necessary to remove the sharp edges to prevent leaks in the membrane at these places.

The corrugations had a width of almost 60 mm. In the mass-transfer experiments no measures were taken to prevent flow around the corrugations along the side wall. In the hydrodynamic study this flow was prevented by applying a foam tape at the side wall of the channel. This reduced the channel width to 42 mm, the channel height remaining 6 mm.

The corrugations were only applied at the side where the membrane was used. The opposite wall remained flat. The application of corrugations at the opposite side also will be the subject of further research.

Membranes

Cellulose acetate membranes were used. Either they were produced in-house or, for mass-transfer studies where a high flux is necessary, the more open membranes produced by Hydranautics were used.

Membrane module

The module in which the membrane was installed consists of two stainless steel parts. In one part a rectangular channel was made with a height of 6 mm and a width of 60 mm. The construction of the feed inlet and outlet of the module transformed the feed stream from circular to rectangular. The flow is led over the membrane as shown in Fig. 1.

Mass-transfer experiments

Mass-transfer studies were performed by varying the velocity in a hyperfiltration module. The resulting fluxes and rejections were used for calculation of the mass-transfer coefficient. The module was placed in a circulation-type installation (Fig. 2). A reciprocating pump was used to feed the system. The

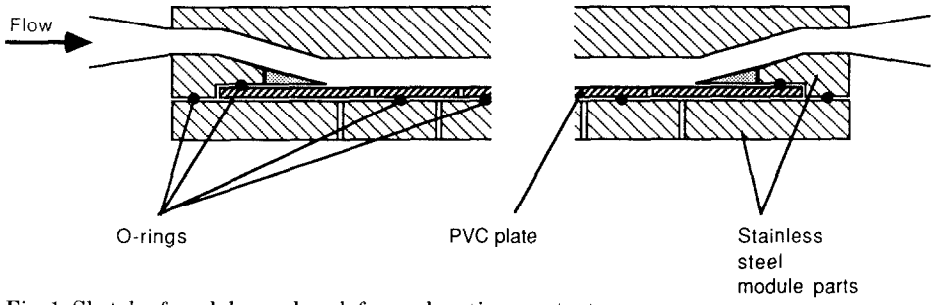

Fig. 1. Sketch of module employed; for explanation, see text.

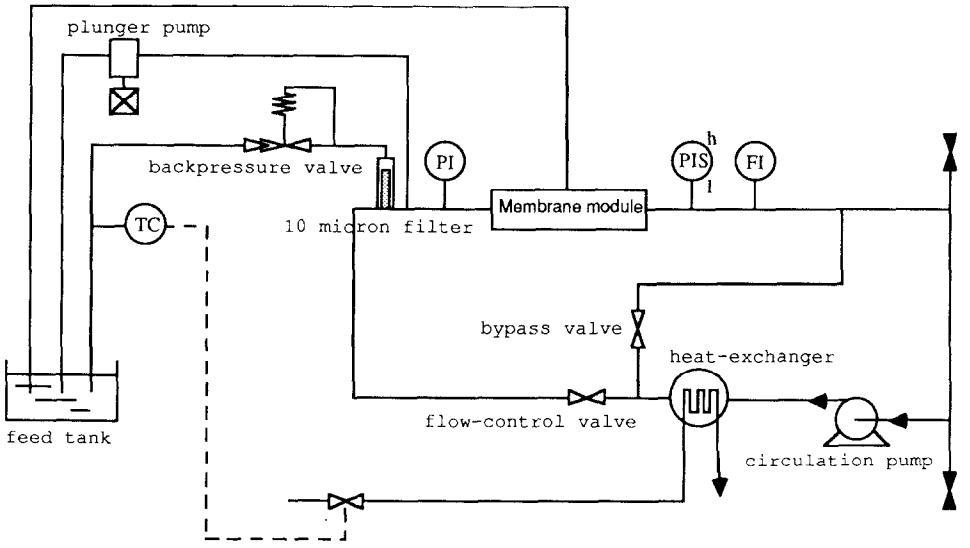

Fig. 2. Flow diagram of membrane filtration installation.

pressure in the loop was controlled by a spring-operated backpressure valve. A circulation pump forced the water to flow through a loop in which the modules were installed. The flow through the module was measured with an electromagnetic flow meter, and manually set with two valves, one of which allows water to flow through a by-pass line. A cartridge filter (nominal 10 μm) was placed in the loop to remove fouling materials. All metal parts of the system were of stainless steel to prevent corrosion. On the flat or corrugated plates a permeate spacer with the same dimensions as the plates was placed. The spacer was locally impregnated with a rubber latex to isolate two rectangles of about 15 cm$\times$3 cm from which permeate was collected separately. The rectangles and the surroundings were connected to small holes to remove permeate. The rectangles were applied to prevent wall effects.

The permeate spacer caused a negligible pressure drop at the permeate side. On top of the permeate spacer a flat membrane with the same dimensions was placed, with the active side away from the spacer. The plate with spacer and membrane was then placed in the stainless steel module. After installing the membrane, the system was filled with water and subsequently pressurized to the working pressure. It is assumed that under ultrafiltration and hyperfiltration conditions the membrane is pressed over the corrugations into the same shape as the corrugated plate. A circulation flow rate was set as well. The system was allowed to operate for at least 16 hours before mass-transfer measurements were performed.

Hydrodynamics

For the hydrodynamic investigations a transparent perspex module was used, identical to the module used for the hyperfiltration experiments. The perspex module was placed in an open loop system (Fig. 3), which was continuously fed with tap water. The overflow of the watertank was sent to a drain. A centrifugal pump delivered water from the tank to the perspex module. A flat or corrugated plate without a membrane was installed in the module.

At the upstream side a hole was drilled in the corrugated plate through which black ink was injected. The ink flow indicated streamlines present in the flow, which could be either laminar or turbulent. The flow was said to be turbulent when streamline irregularities perpendicular to the main flow direction were detected visually.

Two holes in the module at a distance of 37.5 cm were used to measure the pressure drop over this length. The pressure drop was read from a U-tube filled

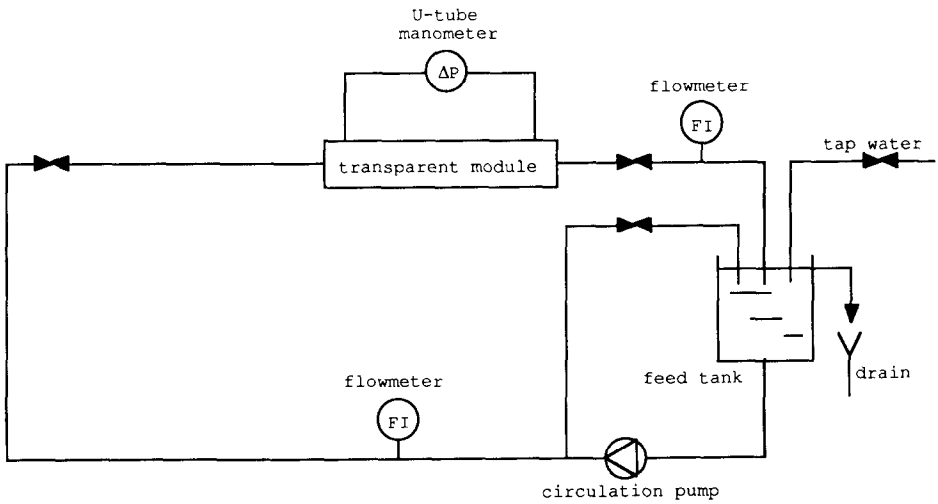

Fig. 3. Flow diagram of installation used in hydrodynamic study.

with the applied tap water. Only when the flow was turbulent, the reading had a value high enough to be determined . The feed flow rate was measured with an electromagnetic flow meter for higher flow values and a float-type flow meter for lower flow values.

Theory and calculation procedure

For the cellulose acetate membranes used it is assumed that the following equations, which are usually applied in hyperfiltration, hold:

$$\textit{water flux: } J_w = A\ (\Delta P - \Delta\pi_w) \tag{1}$$

$$\textit{salt flux: } J_s = B\ (C_w - C_p) \tag{2}$$

in which

$$C_p = J_s / J_w \tag{3}$$

$$\Delta\pi_w = RTi\ (C_w - C_p) \tag{4}$$

These equations hold for hyperfiltration of dilute solutions and independent diffusive flow of water and salt within the membrane.

For the salt concentration near the membrane wall C_w the following equation is used:

$$\frac{C_w - C_p}{C_f - C_p} = \exp\ (J_w / k) \tag{5}$$

This equation results from balancing diffusive and convective flows inside the hydrodynamic boundary layer near the membrane [18].

The above set of equations can be used in design calculations. The values of A and B are assumed to be independent of salt concentration. The same is assumed for the diffusion coefficients in water and the viscosity of the salt solutions within the range of concentrations studied (maximum 20,000 ppm). Based on these assumptions and for a fixed geometry, the mass-transfer coefficient is only dependent on the feed flow velocity.

For values of A and B for a cellulose acetate membrane of 4.0×10^{-12} m/sec-Pa and 2.0×10^{-6} m/sec, respectively (equivalent to 56 l/m^2-hr and 87% rejection at 4 MPa), the curves shown in Fig. 4 can be calculated from eqns. (1)–(5). It is clear that the effect of variation of the mass-transfer coefficient on the membrane performance is rather small for values above 4×10^{-5} m/sec.

Hyperfiltration experiments were carried out at 4 MPa. The feed flow velocity was varied from 0.1 to 2.0 m/sec ($Re = 1{,}000$–$20{,}000$). At five different velocities the corresponding flux and rejection were measured. The temperature was kept constant at 30°C.

For a flat wall, correlations exist in the literature from which the mass-transfer coefficient can be calculated. For corrugated plates no correlation exists

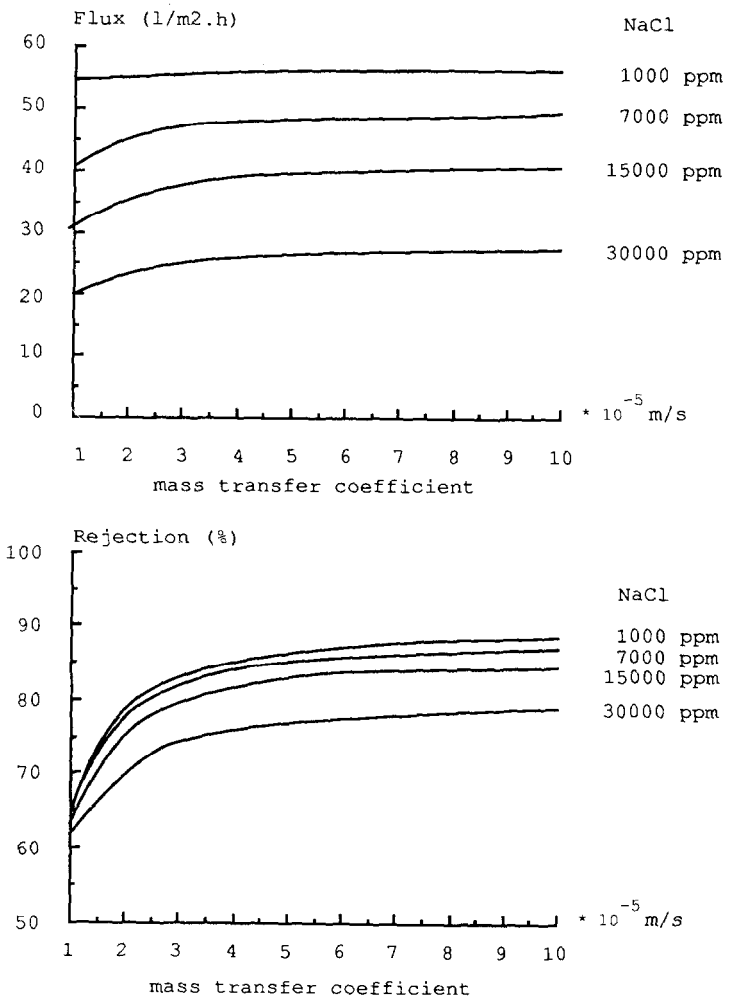

Fig. 4. Calculated flux and rejection as a function of the mass transfer coefficient for a hyperfiltration membrane. $A = 4 \times 10^{-12}$ m/sec-Pa; $B = 2 \times 10^{-6}$ m/sec.

yet. It is the subject of this and following research to find such correlations. Basically, the correlation should be based on distinct values of the mass-transfer coefficient, which should be combined with a mechanistic or semi-empirical mathematical model to give values for the parameters in this model. In this work two methods are used to find distinct values from hyperfiltration data: the "direct" method and a "fitting" method.

"Direct" method

From an experiment without salt in the feed, the value of A can be calculated. The values of B and k can then be calculated from experiments with salt added

to the feed. This calculation is straightforward; however, the variation in B was rather high, whereas sometimes negative values of k were calculated. In the latter case the salt concentration near the membrane wall was calculated to be lower than the concentration in the feed.

These erratic results are caused by the small effects to be measured, but may also be caused by variation of the values of A and B as a function of salt concentration.

"Fitting" method

In order to have the smallest possible variation in the values of A and B, only experiments at a single salt concentration in the feed were used. A method was developed to find values of A, B and k from these experiments. By "trial and error" variation of A, B and each k, values of these variables can be estimated at which the deviation between experimental and calculated fluxes is at a minimum. Because of the algorithm used for varying estimated values of k, no negative values can be calculated. However, sometimes unrealistically high values for the mass-transfer coefficient were found for experiments where a high velocity was used. In this case, the mass-transfer coefficient is thought to be high and so the salt concentration near the membrane wall is almost the same as the concentration in the feed bulk.

More details of the fitting procedure are given in the Appendix.

Results

Deformability of the membrane

After cutting off the sharp edges at the axial ends of the PVC corrugations no leaks were detected for all cellulose acetate membranes used. Despite the expected scatter in the calculated values of A and B, a clear trend follows from Fig. 5. It can be concluded that cellulose acetate membranes can be deformed over corrugated surfaces, provided no sharp edges are present.

Mass transfer

For accurate measurements both the flux and the rejection should be high. For this purpose a relatively open membrane and a bivalent salt were used. First, the commonly applied Na_2SO_4 was used, but it was found that a change in flow velocity caused a reproducible overshoot in the rejection as a function of time. This overshoot can be described by an increase of salt concentration in the permeate after a decrease of flow velocity. The concentration passes through a maximum and reduces then to a stable value, the value being higher than that before the change in velocity. A similar description is valid for an increase in flow velocity. When $CaCl_2$ was used instead, no overshoot reaction was seen. The cause of the overshoot with Na_2SO_4 is not clear. For different feed concentrations, after reaching steady state, constant values for A and B

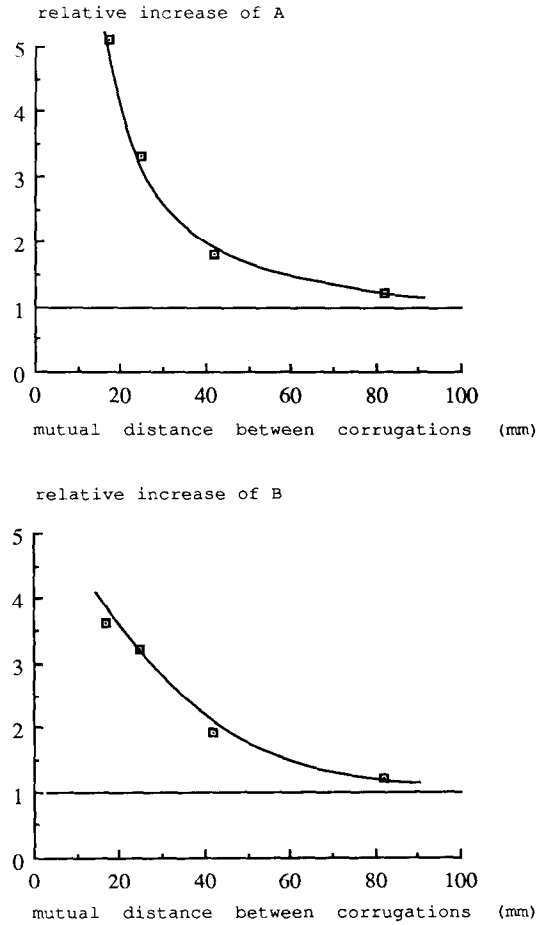

Fig. 5. Relative increase of A and B after application of corrugations to the membrane. Corrugations: half cylinders, height 1.5 mm.

were found for Na_2SO_4 as well. In our opinion, the overshoot reaction can only be explained by changes occurring inside the membrane.

Using experimental data of flux and rejection of flat membranes in the fitting procedure to calculate the mass-transfer coefficient k, values were found which were between 40 and 100% of the values calculated from literature correlations. For separate series the values differed less than 25% from the regression line in a log k versus log U plot. For corrugated membranes the scatter (defined as the deviation from a best straight line fit in a log k–log U plot) increased with increasing mass-transfer coefficient. This may be explained by the relatively small effect on flux and rejection of variation of the mass-transfer coefficient at these high values.

In Fig. 6, a plot of log k versus log U, the results for different corrugated

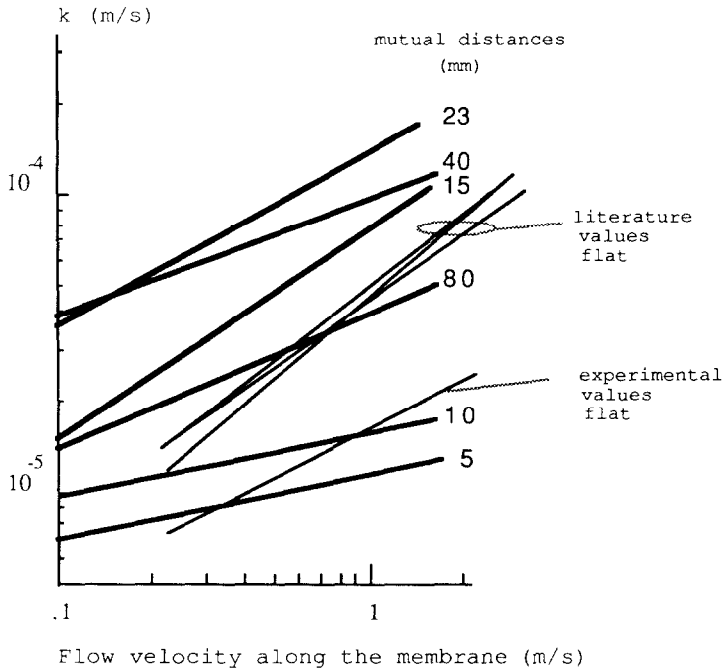

Fig. 6. Mass transfer coefficients for flat and corrugated membranes. Channel dimensions: height 6 mm, width 60 mm. Corrugations: half cylinders, height 1.5 mm.

membranes are given. The values of U and k are based on the geometry of a channel without corrugation. From Fig. 6 it can be concluded that the application of corrugations can improve mass transfer, provided the corrugations are not placed too close together. Mutual distances in the range of about 15–40 mm have the largest effect on mass transfer. Because of low accuracy, for reasons given before, no more precise conclusion can be drawn, despite the clear trend arising in Fig. 6.

Hydrodynamics

In a transparant module having the same dimensions as the stainless steel module used for hyperfiltration experiments, the flow was visualized to get an indication of the form of the streamlines and of the velocity or Reynolds number at which transition takes place from laminar to turbulent flow. For this purpose the flow was defined to be turbulent when irregular deviations of the streamlines were detected perpendicular to the main flow direction. The flow was visualized by injection of black ink through a hole in the corrugated plate. The transition of laminar to turbulent flow occurs for a corrugated plate at a lower velocity than for a flat plate. This transition velocity depends also on the mutual distance. Reynolds numbers corresponding to these velocities, based

TABLE 1

Critical Reynolds numbers for corrugated plates. Corrugations: half-cylinders, 1.5 mm height

Mutual distance (mm)	Critical *Re* (–)
10	870
15	850
23	600
40	850
80	1230
flat	1850

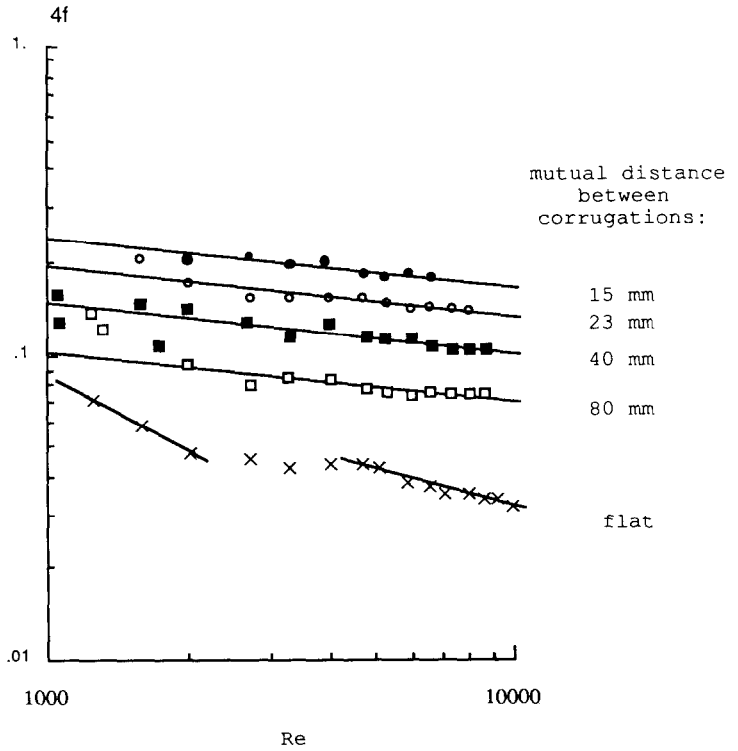

Fig. 7. Friction factor as a function of Reynolds number for flat and corrugated walls. Corrugations at one side of the channel, half cylinders, 1.5 mm height.

on channel dimensions without corrugations, are given in Table 1. For velocities above the transition velocity the pressure drop was high enough to be measured. The values of $4f$, calculated from the formula for the pressure drop

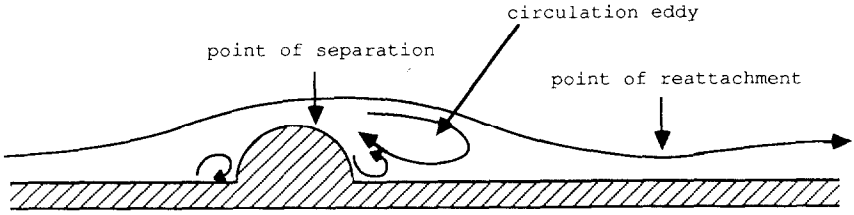

Fig. 8. Impression of streamlines for flow over corrugated plates.

$$\Delta p = 4f \tfrac{1}{2}\rho U^2 \frac{L}{d_h}$$

are plotted as a function of the Reynolds number in Fig. 7. It is clear that for all given corrugated plates the pressure drop is higher compared with the pressure drop of a flat plate.

Both in laminar and turbulent flow a circulation behind the corrugation was visible. A sketch of the streamlines is given in Fig. 8. The circulation reaches to about 10–15 mm behind the corrugation. When the mutual distance of the corrugations was less than this value, a circulation was found that filled the whole space between the corrugations, while the streamlines of the main flow did not reach the plate.

When ink was continuously injected into this circulation in a laminar flow a broad line of ink could be produced starting somewhere on the corrugation — likely the so-called stagnation point where the ongoing steamlines detached from the fixed wall — and continuing throughout the module. After stopping the ink injection the black color disappeared slowly, starting from the point where the ongoing streamlines are believed to reattach to the fixed wall. Rather surprisingly, ink disappeared also relatively fast from the circulating zone. In the small rectangular corner between the plate and the corrugation a small black spot remained rather long, indicating a stagnant spot. Changing the shape of the corrugation could solve this problem.

Energy consumption as a function of the mass-transfer coefficient with corrugated plates

At the same flow velocity, corrugated plates have a larger pressure drop than flat plates. However, mass transfer is increased if appropriate mutual distances are used. A comparison of Figs. 6 and 7 allows for a quick determination whether a corrugated or a flat plate should be used to realize a more energy-efficient mass transfer. The results for the four corrugated plates with the highest mass transfer are given in Fig. 9. At a given mass-transfer coefficient, the application of corrugated plates can lead to a lower energy consumption. Figure 9, however, should be interpreted with care. Because of experimental uncertainties, the

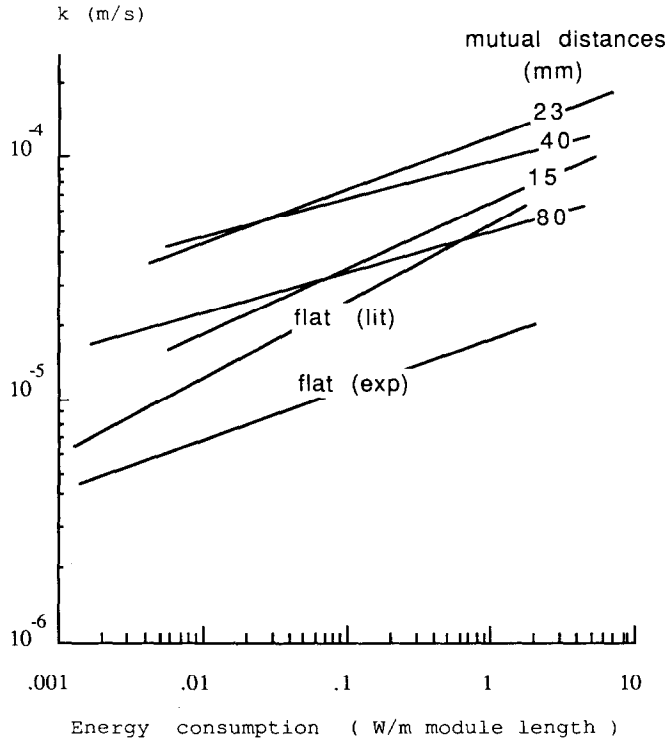

Fig. 9. Energy consumption of flat and corrugated membrane modules. Corrugations: half cylinders, height 1.5 mm. Channel dimensions: height 6 mm; width 60 mm.

lines obtained are only good estimates for the mass transfer coefficient. A mutual distance of 23 mm seems to be optimal.

Pressure drop as a function of the mass-transfer coefficient with corrugated plates

For circulation systems it is important to know the energy consumption for any desired value of the mass-transfer coefficient. When corrugations cause a high pressure drop, less modules are placed in series and more in parallel. For once-through systems not the energy consumption but the pressure drop belonging to a desired value of the mass-transfer coefficient is the determining factor. For a value for the mass-transfer coefficient of 4×10^{-5} m/sec the corresponding pressure drop can be read off from Figs. 6 and 7.

For mutual corrugation distances of 15, 23, 40, 80 mm and for a flat plate, pressure drops are calculated to be 2200, 190, 100, 4500 and 2000 Pa/m, respectively. Again the mutual distances of 23 and 40 mm are seen to be the best ones. This conclusion also should be used with care because of the mentioned experimental uncertainties.

Discussion

The existence of a mutual distance where the increase in mass-transfer is at a maximum can partially be explained by the shape of the streamlines shown in Fig. 8. Assuming that the local mass transfer is most enhanced at the point where the ongoing streamlines reattach again to the wall, a region exists around this point where the mass transfer is also, but at a lesser degree, enhanced. If only one corrugation exists, far downstream the situation will be the same as for a flat plate. Going from the point of reattachment back to the corrugation it is expected that the local mass transfer decreases to values lower than for a flat plate. This supposition is based on the low rate of refreshment in the rectangular corner downstream of the corrugation, seen in the hydrodynamic study. The point of reattachment was found to be at a distance of 10 to up to 15 mm from the corrugation. For smaller mutual distances the magnitude of enhancement is expected to decrease, as indeed found. For larger mutual distances it can be expected that the magnitude of enhancement reduces too. From the results given in Fig. 6, it is seen that only for a distance above 40 mm a reduction of the enhancement is found.

These arguments are in accordance with the conclusions of Focke [19], who measured in a comparable system the local mass transfer electrochemically. Besides a small region of enhancement upstream of and on the promoter, a maximum in mass transfer was found at some distance downstream. This downstream enhancement is probably caused by an increase in turbulence, as concluded from the local fluctuations in mass transfer. Focke also detected an increase in mass transfer at the wall not equipped with the promoter. From the geometry and local fluctuations he concludes that this enhancement is caused by flow acceleration and by increase in turbulence. The latter may even result from flow separation downstream of the corrugation at the non-corrugated wall [19].

The existence of an increase in turbulence was experimentally determined by Hijikata and Mori [20] with a laser Doppler velocimeter. After separation of the (turbulent) flow on top of the corrugation a sharp local increase in turbulence is detected. This increased turbulence "diffuses" sidewards, and around the reattachment point the turbulence causes an increase in mixing near the wall, thereby increasing the local heat or mass transfer.

Zukauskas and Pedisius [24] found a dependence of the location of maximum heat transfer downstream of a corrugation on the value of the Prandtl number. This can be explained by the diffusive penetration of the turbulence into the boundary layer. The value of the Prandtl number in heat transfer and the Schmidt number in mass transfer determines which part of the hydrodynamic boundary layer plays a determing role in the heat or mass transfer process.

Fischl et al. [25] found in an electrochemical cell with obstacles attached or

detached an optimal spacing of approximately 15 times the obstacle size. Given the 1.5 mm corrugation height used in this work, an optimal corrugation spacing of 23 mm would result, which is in accordance with our findings.

Miyashita et al. [21] found a maximum enhancement of the mass transfer behind a cylindrical turbulence promoter at a distance of 5–8 times the promoter size. The maximum coincides with "violent fluctuations in the flow near the wall". Behind this point of maximum enhancement, the local mass transfer was found to decrease to values corresponding to an unobstructed channel. Local mass transfer for obstacles attached to the wall were also measured by Leitz and Marincic [22], and Storck and Hutin [23]. All of them found a maximum enhancement of the mass transfer at some distance behind the corrugation.

From Fig. 9 it follows that for some of the corrugated plates studied a given value of the mass transfer coefficient k can be realized with a reduced energy consumption. Storck and Hutin [26] studied several different turbulence promoters and calculated the same type of curves for these promoters as given in Fig. 9. At the same energy consumption a difference in k value of a factor of 2 can be read from their plot, whereas at the same k value a difference in energy dissipation of a factor of 20 is found. Storck and Hutin concluded that all turbulence promoters are energetically equivalent within a range of 50%, despite the fact that some systems give better performance than others. For their work, and from the results given in this work, a more detailed conclusion can be drawn. The application of a rigid turbulence promoter may be energetically advantageous when the promoter is as close as possible to the active wall, or preferably, is part of the active wall itself.

Mixing or flow deformation, necessary for enhancement of mass transfer, should mainly occur near the wall, inside the mass transfer boundary layer. So, rigid obstructions placed in the middle of a channel are expected to be less energy efficient than obstructions at or inside of the active wall. Moreover, from this work it is seen that for obstructions at or inside the wall a correct arrangement is necessary for energy effectiveness.

Acknowledgement

These investigations were supported in part by the Netherlands Foundation for the Technical Sciences (STW), the future Technical Science Branch of the Netherlands Organization for the Advancement of Pure Research (ZWO). E. Löbker and H. Kranenberg cooperated in this research to fullfil the requirements for finishing their HTS education. K.J. Hutter also cooperated to fullfil the requirements for his M.Sc. thesis. Technical assistance was given by A.G. Rooks.

List of symbols

A permeability constant for water flux (m-sec^{-1}-Pa^{-1})
B permeability constant for salt flux (m-sec^{-1})
C concentration (kmol-m^{-3})
d_h hydraulic diameter (m)
f friction factor (–)
i number of ions per molecule (–)
J flux of component (m-sec^{-1})
k mass transfer coefficient (m-sec^{-1})
L module length (m)
Δp pressure drop along module (Pa)
ΔP pressure difference over membrane (Pa)
R gas constant (8.314 kJ-mol^{-1}-K^{-1})
T temperature (K)
U flow velocity (m-sec^{-1})
$\Delta \pi$ osmotic pressure difference over membrane (Pa)
ρ density (kg-m^{-3})

Subscripts
f feed
p permeate
s salt
w wall

References

1 P. Dejmek, B. Funeteg, B. Hallström and L. Winge, Turbulence promoters in ultrafiltration of whey protein concentrate, J. Food Sci., 39 (1974) 1014–1017.
2 J. Murkes and H. Bohman, Mathematical modelling of reverse osmosis and ultrafiltration processes, Desalination, 11 (1972) 269–301.
3 E.W. Pitera and S. Middleman, Convection promotion in tubular desalination membranes, Ind. Eng. Chem., Process Des. Dev., 12 (1) (1973) 52–56.
4 J. Hiddink, D. Kloosterboer and S. Bruin, Evaluation of static mixers as convection promoters in the ultrafiltration of dairy liquids, Desalination, 35 (1980) 149–167.
5 A.L. Copas and S. Middleman, Use of convection promotion in the ultrafiltration of a gel-forming solute, Ind. Eng. Chem., Process Des. Dev., 13 (2) (1974) 143–145.
6 D.G. Thomas, P.H. Hayes, W.R. Mixon, J.D. Sheppard, W.L. Griffith and R.M. Keller, Turbulence promoters for hyperfiltration with dynamic membranes, Environ. Sci. Technol., 4 (12) (1970) 1129–1136.
7 J.S.S. Shen and R.F. Probstein, Turbulence promotion and hydrodynamic optimalization in an ultrafiltration process, Ind. Eng. Chem., Process Des. Dev., 18 (3) (1979) 547–554.
8 J. Csurny, J.S. Johnson, K.A. Kraus, H.O. Philips, W.G. Sisson and C.G. Westmoreland, in: G.E. Moore and J.S. Johnson Jr. (Eds.), Biennial Progress Report for the Period 15/3/1968–15/3/1970, Oak Ridge National Laboratory, Oak Ridge, Tennessee, 1973, p. 270.
9 J. Lai, Ph.D. Thesis, Montana State University, Bozeman, Montana, 1971, MD 409 a 025.

10 H. Lolachi, Fluidized bed in reverse osmosis processes, O.S.W. R&D Res. Dev. Rep. No. 843, U.S. Dept. of Interior, 1973; U.S. Patent Appl. 446,833, 1974.
11 M.J. van der Waal, P.M. van der Velden, J. Koning, C.A. Smolders and W.P.M. van Swaaij, Use of fluidised beds as turbulence promoters in tubular membrane systems, Desalination, 22 (1977) 465-483.
12 R. de Boer, J.J. Zomerman, J. Hiddink, J. Aufderheyde, W.P.M. van Swaaij and C.A. Smolders, Fluidized beds as turbulence promotors in the concentration of food liquids by reverse osmosis, J. Food Sci., 45 (1980) 1522-1528.
13 W.G. Light and T.V. Tran, Improvement of thin-channel design for pressure-driven membrane systems, Ind. Eng. Chem., Process Des. Dev., 21 (1981) 33-40.
14 G. Schock and A. Miguel, Druckverlust und Stoffaustausch in Wickelmodulen, Preprints Aachener Membran Kolloquium, 16-18 March 1987, Aachen, 1987, pp. 89-102.
15 H. Rybinova, Contribution to the problem of heat transfer and pressure drop in plate heat exchangers, Verfahrenstechnik 4 (9) (1970) 413-416.
16 R. Koch, Druckverlust und Wärmeübergang bei verwirbelter Strömung, VDI Forschungsheft, 469 (24) (1958) 395-403.
17 I.G. Racz, J. Groot Wassink and R. Klaassen, Mass transfer, fluid flow and membrane properties in flat and corrugated plate hyperfiltration modules, Desalination, 60 (1986) 213-222.
18 P.L.T. Brian, Mass transport in reverse osmosis, in: U. Merten (Ed.), Desalination by Reverse Osmosis, MIT Press, Cambridge, MA, 1966, p. 161.
19 W.W. Focke, On the mechanism of transfer enhancement by eddy promoters, Electrochim. Acta, 28 (8) (1983) 1137-1146.
20 K. Hijikata and Y. Mori, Fundamental study of heat transfer augmentation of tube inside surface by cascade smooth surface-turbulence promoters, Wärme- Stoffübertrag., 21 (1987) 115-124.
21 H. Miyashita, A. Takayanagi, Y. Shiomi and K. Wakabayashi, Flow behavior and augmentation of the mass transfer rate in a rectangular duct with a turbulence promoter, Int. Chem. Eng., 4 (1981) 646-651.
22 F.B. Leitz and L. Marincic, Enhanced mass transfer in electrochemical cells using turbulence promoters, J. Appl. Electrochem., 7 (1977) 473-848.
23 A. Storck and D. Hutin, Mass transfer and pressure drop performance of turbulence promoters in electrochemical cells, Electrochim. Acta, 26 (1980) 127-137.
24 A. Zukauskas and A. Pedisius, Heat transfer to reattached fluid flow downstream of a fence, Wärme- Stoffübertrag., 21 (1987) 125-131.
25 D.S. Fischl, K.J. Hanson, R.H. Muller and C.W. Tobias, Mass transfer enhancement by small flow obstacles in electrochemical cells, Chem. Eng. Commun., 38 (1984) 191-207.
26 A. Storck and D. Hutin, Energetic aspects of turbulence promotion applied to electrolysis processes, Can. J. Chem. Eng., 58 (1980) 92-102.

Appendix

Description of the fitting procedure to obtain A, B *and* k *from experiments at one salt concentration*

In eqns. (1)-(5), which describe the fluxes of water and salt as a function of the process conditions, 13 variables exist, of which R, T and i are known and ΔP, J_w, C_f and C_p are determined experimentally, so that for one experiment there are 12 equations for the 13 variables.

It is assumed that A and B are the same for every experiment with the same membrane. With this condition, 8 extra variables occur for each next experi-

ment as well as 9 extra equations (5 basic equations and ΔP, J_w, C_f and C_p values). Combining two experiments, a set of equations results that can be solved mathematically. Because of experimental uncertainties, usually a set of equations belonging to about five experiments is numerically elaborated instead of a set of equations arising from two experiments. This set of equations is over-determined, but because of experimental uncertainties deviations between experimental and calculated fluxes are allowed. Now by "trial and error" variation of A, B and each k the values of these variables can be estimated at which the deviation between experimental and calculated fluxes is at a minimum. The "trial and error" variation was performed with a standard minimisation procedure. In fact the estimation procedure was a two-step operation: for each estimate of values of A and B the best value of each k was estimated and the deviation between experiment and calculation determined. Based on this deviation value other values of A and B were estimated. The procedure can be applied even at different feed concentrations for each experiment, provided the values of A and B can be assumed constant.